Augmented optimal LQR control system design for the longitudinal flight dynamics of an UAV: Inner and outer loop concepts

KAMURAN TURKOGLU [1] ELBROUS M. JAFAROV [2]
Department of Aeronautics and Astronautics,
Istanbul Technical University, Istanbul, Turkey
Istanbul Teknik Universitesi, Ucak-Uzay Bilimleri Fakultesi, Maslak 34469, Sariyer, Istanbul
TURKEY

Abstract: - In this paper, an augmented optimal LQR control system design procedure has been implemented on the longitudinal flight dynamics of a theoretical UAV, which has been studied in Faculty of Aeronautics and Astronautics of Istanbul Technical University. Throughout the dynamic modeling, open loop dynamics has been investigated and the modes of the longitudinal flight have been inspected. Concerning the open loop time domain responses, an augmented LQR control system design has been applied on the system dynamics. It has been observed that the lightly damped mode could be suppressed in a great manner. In addition, remarkable settling time and actuator signal values has been achieved. Computer simulations show the effectiveness of the proposed approach.

Key-Words: - UAV, Longitudinal Dynamics, Optimal Control, LQR, Augmented Plant

1 Introduction

Control system design of small and inexpensive Unmanned Aerial Vehicles (UAVs) is of great interest in military and civilian applications, including mapping, patrolling, search and rescue. These tasks sometimes could be dangerous and recurring, which makes them ideal for autonomous vehicles [1]. In these types of applications, control system design, as well as dynamic modeling, has a crucial role in the behavior of the UAV and in mission accomplishment. Therefore it is vital to gain knowledge about dynamic properties of the UAV in order to be used in control system design procedure. In literature, there are several conducted researches on automatic control system designs of UAVs such as receding horizon control [2], variable horizon model predictive control [3], control system design using evolutionary algorithms [4], feedback linearization and linear observer design [5], cooperative receding horizon control [6], adaptive control system design [7], control system design using MIMO QFT [8], decentralized non-linear control [9], robust control system design using coupled stabilities [10], H infinity control and inverse dynamic system approach [11] and non-linear autopilot design using dynamic inversion [12], are some of the studies.

In this study, as a different approach to the existing studies, an augmented Optimal Linear Quadratic Regulator (LQR) control design procedure, taken from [13], has been used for the control system design of an UAV in longitudinal flight regime. As a first step, longitudinal dynamics of the UAV have been derived and open loop time domain responses have been analyzed. According to the open loop time domain responses, required control algorithms have been considered with respect to the necessities of the open loop dynamics. For this purpose an augmented LQR control system model, taken from [13], has been implemented on the longitudinal flight dynamics of the UAV and obtained results have been given in details in the following sections.

2 Longitudinal dynamics of UAV

Before getting into the control system design, in the second section of the paper, longitudinal flight characteristics have been obtained. In order to that Equations of Motion (EOMs) governing the longitudinal flight, taken from [14], has been used for analysis and are given in (1) as

$$
\begin{aligned}
&\boldsymbol{x:}\quad (\frac{mu}{Sq}s - C_{X_u})'u(s) - C_{X_\alpha}{}'\alpha(s) - C_{W}(\cos\Theta)\theta(s) = 0 \\
&\boldsymbol{z:}\quad -C_{Z_U}{}'u(s) + \left[(\frac{mu}{Sq} - \frac{c.C_{Z\dot{\alpha}}}{2u})s - C_{Z_\alpha}\right]'\alpha(s) \qquad (1) \\
&\quad + \left[(-\frac{mu}{Sq} - \frac{c.C_{Zq}}{2u})s - C_W \sin\Theta\right]\theta(s) = 0 \\
&\boldsymbol{M:}\ (-\frac{c.C_{m_{\dot{\alpha}}}}{2u}s - C_{M_\alpha})'\alpha(s) + (\frac{I_y}{Sqc}s^2 - \frac{c.C_{M_q}}{2u}s)\theta(s) = 0
\end{aligned}
$$

where

$'u$ = change of velocity in longitudinal flight
$'\alpha$ = change of angle of attack in longitudinal flight
θ = change of pitch angle from equilibrium point

and

$$'u = \frac{u}{U_0} \quad , \quad '\alpha = \frac{w}{U_0}$$

where

u = velocity in X direction
w = velocity in Z direction

After the introduction of EOMs, characteristic properties of UAV have been calculated and found as shown in Table-1 and Table-2, respectively [15].

Table 1 Characteristic properties of UAV.

m =	5 [kg]
$\mathbf{U_0}$ =	12 [m/sec]
g =	9.807 [m/sec^2]
$\mathbf{S_{wing}}$ =	0.4205 [m^2]
$\mathbf{S_{vertical\ tail}}$ =	0.1323 [m^2]
ρ =	1.226 [kg/m^3]
$\mathbf{I_{yy}}$ =	0.1204 [m^4]
c =	0.235 [m]

Table 2 Stability derivatives and inputs of UAV.

$C_{x_u} = -0.0264$	$C_{Z_{\dot{\alpha}}} = -0.0347$
$C_{x_\alpha} = 1.2821$	$C_{Z_\alpha} = -0.1381$
$C_D = 0.0132$	$C_{Z_q} = -3.30$
$C_L = 1.3210$	$C_{M_{\dot{\alpha}}} = -0.0347$
$C_W = -1.3210$	$C_{M_\alpha} = -0.0312$
$L_{t/c} = 1$	$C_{M_q} = -3.30$
$C_{Z_u} = -2.6421$	$C_{X_{\delta_e}} = 0$
$C_{Z_{\delta_e}} = -0.71$	$C_{m_{\delta_e}} = -0.71$

Since we are only interested with the change of pitch angle (θ) with respect to a given elevator deflection (δ_e) in longitudinal flight, only the θ / δ_e transfer function (TF) will be taken into consideration.

Using the characteristic properties and calculated stability derivatives, it is possible to construct the nominal plant representation of θ / δ_e TF as the followings:

$$\frac{\theta(s)}{\delta_e(s)} = \frac{1.858\,s^2 + 0.1531\,s + 2.411}{0.036\,s^4 + 0.089\,s^3 + 0.135\,s^2 + 0.112\,s + 0.109} \quad (2)$$

Also the corresponding modes in longitudinal flight and their characteristics properties could be simply defined as shown in (3).

phugoid mode	**short period mode**
$\xi_{pm} = 0.0147$	$\xi_{sp} = 0.7805$
$\omega_{n\_pm} = 1.1152\ rad/s$	$\omega_{n\_sp} = 1.5580\ rad/s$
$T_{pm} = 61.1027\ s$	$T_{sp} = 0.8223\ s$

(3)

As it is possible to see from both the short period and phugoid mode properties, UAV is lightly damped (under-damped) in phugoid mode, which should be improved in control system design, while the damping ratio in the short period mode is considerably good.

After having an insight related with the open loop dynamics of the UAV, it is also possible to have a look at the frequency domain response of open loops dynamics. Therefore, Bode plot of θ / δ_e TF has been plotted and is presented in Figure-1.

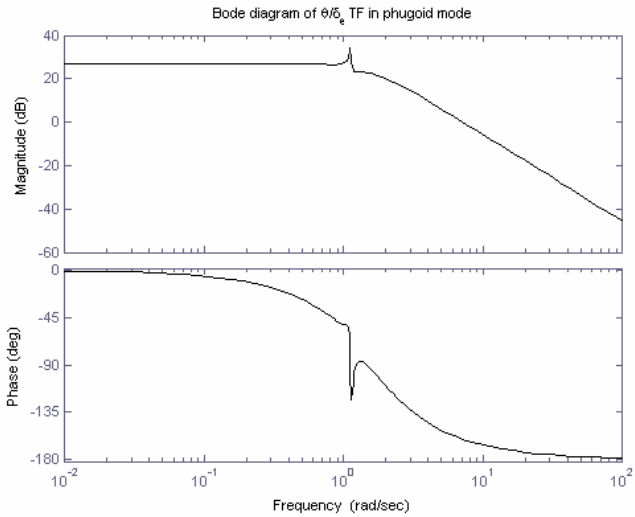

Figure-1 Frequency domain response of θ / δ_e TF.

As it is also possible to see from Figure-1, phugoid mode dynamics ($\omega_{n\_pm} = 1.1152\ rad/s$) are affected in a great manner for a given δ_e deflection. Furthermore, if the open loop time domain responses of θ / δ_e TF is plotted, it is probable to detect the responses as given in Figure-2, where Figure-2 represents the open loop (OL) time domain *step* response and the OL time domain *impulse* response of θ / δ_e, respectively.

From Figure-2, it is straightforward to see the low damping and the long lasting oscillations in the longitudinal flight of Hezarfen UAV system. Due to all specified reasons, a nicely augmented control system design is significantly required in Hezarfen UAV longitudinal flight dynamics.

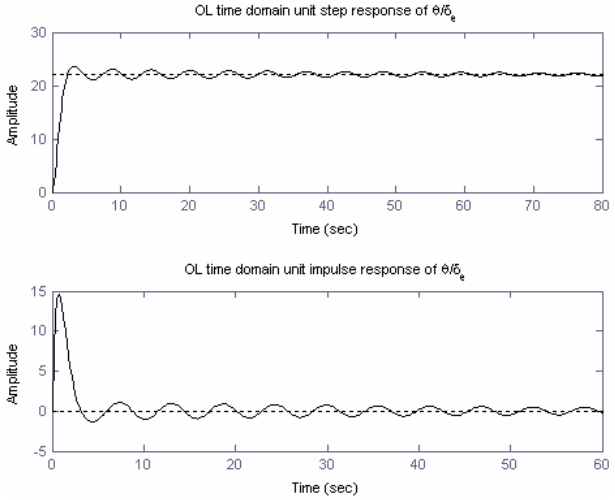

Figure-2 OL time domain responses of θ / δ_e TF.

For the specified reasons, in the following section an augmented optimal LQR control system will be applied to the longitudinal flight dynamics of the UAV in order to have better time domain responses in the system.

3 Controllability and observability

During the control system design process, which is going to be presented in the next section, an observer scheme will be used in order to estimate the outputs those may not be measured during the flight. And just before getting into the control system design part, the observability and the controllability characteristics of the UAV system will be investigated in the followings. Observability matrix of a system is defined as

$$Obs = O_n = \begin{bmatrix} C \\ CA \\ \vdots \\ CA^{n-1} \end{bmatrix} \qquad (3)$$

in [16] and in the light of the observability matrix, a system is described observable if

$$N(O) = \{0\}; \quad i.e.\ Rank(O) = n \qquad (4)$$

And if (3) and (4) are applied in system dynamics, obtained results are being as

$$Obs = O_n \Rightarrow A_{nxn} \ \ and \ \ C_{1xn} \qquad (5)$$

$$\begin{bmatrix} C \\ CA \\ \vdots \\ CA^{n-1} \end{bmatrix} = \begin{bmatrix} 0 & 51.3858 & 4.23 & 66.67 \\ 51.38 & 4.2333 & 66.67 & 0 \\ -122.4 & -126.04 & -159.51 & -155.12 \\ 175.71 & 299.65 & 224.91 & 369.57 \end{bmatrix}$$

$$Rank(O_n) = 4 = n$$

which indicates that our system is fully observable. As a confirmation, it is also possible to calculate the *number of unobservable* states from

$$UnOb = Length(A_{nxn}) - Rank(O_n) \qquad (6)$$

which is also equal to

$$UnOb = Length(A_{nxn}) - Rank(O_n) = 0 \qquad (7)$$

which simply states that we have no *unobservable states* (i.e. all of our states could be observed). Thus, it is feasible to verify that we are able to use an observer for our OL dynamics in longitudinal flight. Additionally, controllability of the system dynamics should be verified, so that there will be no theoretical obstacle to get into the optimal control system design process.

It is also known that the controllability matrix of a system is defined in [16] as

$$A_{nxn} \ \Rightarrow \ C_t = \begin{bmatrix} B & AB & \dots & A^{n-1}B \end{bmatrix} \qquad (8)$$

so that the controllability matrix must satisfy

$$Rank(C_t) = n \qquad (9)$$

condition (9) and in this way the system is called *reachable* or *controllable*. If we apply the given controllability conditions to our system, the results are obtained as

$$C_t = \begin{bmatrix} 1.0000 & -2.4649 & 2.3250 & 0.4097 \\ 0 & 1.0000 & -2.4649 & 2.3250 \\ 0 & 0 & 1.0000 & -2.4649 \\ 0 & 0 & 0 & 1.0000 \end{bmatrix} \qquad (10)$$

$$Rank(C_t) = 4 = n$$

With such observability and controllability analyses, it has been proved that the longitudinal UAV system is both controllable and observable, which grants the opportunity to use an observer in the control system design process.

4 LQR control system design

In this section of the paper, an optimal LQR control system design, taken from [13], will be implemented on the OL system dynamics. During the procedure, inner loop and outer loop concepts has been used in the design, where inner loop has been used to reach considerable stability characteristics and outer loop has been used for significant performance distinctiveness.

First of all, the Simulink block diagram has been constructed for simulation purposes and has been obtained as shown in Figure-3.

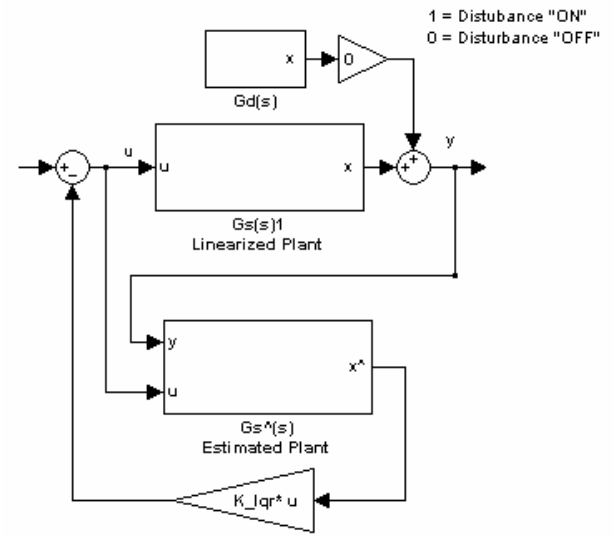

Figure-3 Simulink block diagram of inner loop.

Here, the linearized plant dynamics ($G_s(s)$) has been represented with the actuator (elevator) servo mechanism as shown in Figure-4a and estimated ($\hat{G}_s(s)$) plant dynamics has been represented as shown in Figure-4b.

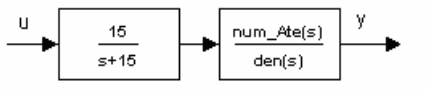

Figure-4a Simulink block diagram of $G_s(s)$.

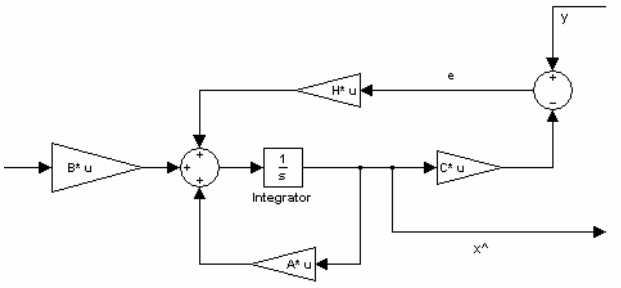

Figure-4b Simulink block diagram of $\hat{G}_s(s)$.

H (pole placing weighting matrix in observer) has been selected in a way so that the poles of the observed system could be like

$$eig(Observer) = \begin{bmatrix} -15.0000 \\ -1.7925 + 1.1873i \\ -1.7925 - 1.1873i \\ -0.7070 + 0.7072i \\ -0.7070 - 0.7072i \end{bmatrix}$$

while

$$H = \begin{bmatrix} 0.0407 & -0.0445 & -0.0327 & 0.0371 & 0.0254 \end{bmatrix}$$

This construction has been defined as the inner loop and has been mainly considered for the stability purposes in the plant. The outer loop of the plant has been constructed using the K_I, K_{filter} gains and a filter $(1/s)$. But also, for the outer loop concept, state space system matrixes (A, B, C, D) have been augmented in order to have appropriate weighting in the system. The augmentation of the system matrixes has been conducted as the followings:

$$A_{aug} = \begin{bmatrix} 0 & \vdots & -C \\ \cdots & \cdots & \cdots \\ 0 & \vdots & \\ 0 & \vdots & \\ 0 & \vdots & A \\ 0 & \vdots & \\ 0 & \vdots & \end{bmatrix}, \quad B_{aug} = \begin{bmatrix} 0 \\ \cdots \\ B \end{bmatrix}, \qquad (11)$$

$$C_{aug} = \begin{bmatrix} \gamma & \vdots & C \end{bmatrix} \text{ where } \gamma \text{ is a scalar gain}$$

After augmenting the system matrixes, the LQR control system design has been obtained using the lqr MATLAB command. Weighting matrixes (*Q and R*), existing in the cost minimization function,

$$J = \int_0^\infty (x^T Q x + u^T R u) dt$$

are selected as

$$Q = diag([\ 1 \quad 1 \quad 200 \quad 200 \quad 20 \quad 20\ ])$$

$$R = 0.38 \quad and \quad \gamma = 10$$

Using the given selections, K-gain matrix (which minimizes the cost function and leads to an optimal design), S-solution of the associated Riccati equation and E-closed loop eigen-values (obtained with $A_{aug} - B_{aug} K_{LQR}$) are calculated as

$$K_{LQR} = \begin{bmatrix} -1.62 & 6.60 & 135.96 & 648.43 & 236.16 & 821.21 \end{bmatrix}$$

$$S = 1e4 * \begin{bmatrix} 0.0001 & -0.0001 & -0.0015 & -0.0109 & -0.0025 & -0.0142 \\ -0.0001 & 0.0003 & 0.0052 & 0.0246 & 0.0090 & 0.0312 \\ -0.0015 & 0.0052 & 0.1100 & 0.5516 & 0.1934 & 0.7010 \\ -0.0109 & 0.0246 & 0.5516 & 3.3231 & 1.0466 & 4.2634 \\ -0.0025 & 0.0090 & 0.1934 & 1.0466 & 0.7173 & 1.3470 \\ -0.0142 & 0.0312 & 0.7010 & 4.2634 & 1.3470 & 5.9530 \end{bmatrix}$$

$$E = \begin{bmatrix} -15.00 \\ -4.54 \\ -2.21+3.66i \\ -2.21-3.66i \\ -0.04+1.13i \\ -0.04-1.13i \end{bmatrix}$$

As a further step, it is possible to extract the K_{filter} gain from obtained K_{LQR} gain such as $K_{filter} = K_{LQR}(1,1) = -1.62$ and the K_I gain is obtained as $K_I = -(C(A - BK_{LQR})^{-1})^{-1} = 0.8664$. After calculating and obtaining the necessary values for the augmented optimal LQR control system design procedure, the simulink block diagram for the augmented system has been constructed and is given in Figure-5.

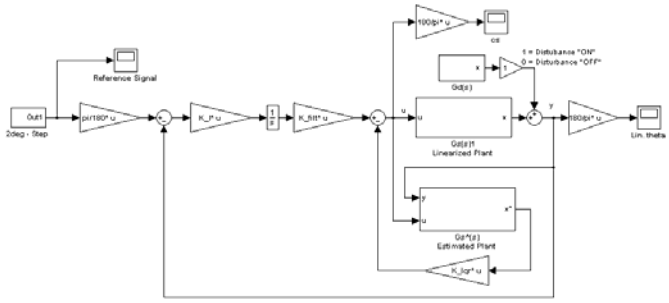

Figure-5 Simulink block diagram of augmented LQR control system (outer loop).

Now it is time to analyze the close loop time domain result of our designed augmented optimal LQR control system design. If we plot the closed loop (CL) time domain results for a given 2 degree elevator deflection, obtained results are shown in Figure-6.

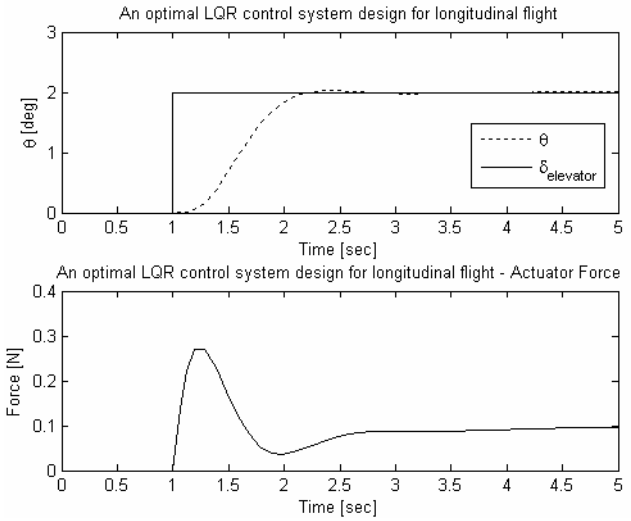

Figure-6 CL time domain results of LQR design.

As it is also likely to see from Figure-6, the settling time is nearly 1.8 second and the maximum actuator effort (force) is approximately 0.3 Newton, which are significant values for a control system design. Moreover, if we check the *tracking* and the *disturbance rejection* of the system with respect to a given 25% disturbance of the input, we obtain such results as given in Figure-7.

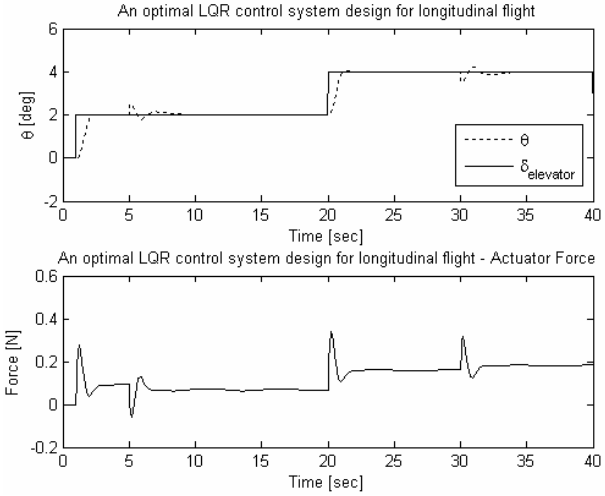

Figure-7 Tracking and disturbance rejection of LQR design.

From Figure-7, it is possible to see that the signal tracking of the augmented LQR control system design is respectable and the disturbance rejection to a given 25% of disturbance is within the acceptable limits.

5 Conclusion

In the paper the longitudinal dynamics of an UAV have been considered and in order to compensate the lightly damped phugoid mode, an augmented optimal LQR control system design has been implemented to the system dynamics. From the closed loop time domain results, it is likely to see that the augmented optimal LQR control system design is able to shape the open loop dynamics so that the settling time is ~1.8 second and the actuator force acting on the elevators is ~0.3 Newton, which are great performance specifications regarding the open loop dynamics.

Acknowledgement

The first author is supported by The Scientific and Technological Research Council of Turkey (TUBITAK) during his Master of Science studies in Istanbul Technical University, Istanbul, Turkey, and would like to express his gratitude towards the support.

References:

[1] Ryan, A., Zennaro, M., Howel, A., Sengupta, R. and Hedrick, J.K., An Overview of Emerging Results Cooperative UAV Control, *43rd IEEE Conference on Decision and Control*, December 14-17, 2004, Atlantis, Paradise Island, Bahamas.

[2] Keviczky, T. and Balas, G.J., Software-enabled receding horizon control for autonomous unmanned aerial vehicle guidance, *Journal of Guidance Control and Dynamics*, Vol. 29, No. 3, 2006, pp.680-694.

[3] Richards, A. and How, J.P., Robust variable horizon model predictive control for vehicle maneuvering, *International Journal of Robust and Non-Linear Control*, Vol.16, No.7, 2006, pp.333-351.

[4] Khantsis, S. and Bourmistrova, A., UAV controller design using evolutionary algorithms, *Advances in Artificial Intelligence Lecture Notes in Artificial Intelligence*, No.3809, 2005, pp.1025-1030.

[5] Mokhtari A., M'Sirdi N.K., Meghriche K. and Belaidi A., Feedback linearization and linear observer for a quadrotor unmanned aerial vehicle, *Advanced Robotics*, Vol.20, No.1, 2006, pp.71-91.

[6] Li, W. and Cassandras, C.G., A cooperative receding horizon controller for multivehicle uncertain environments, *IEEE Transactions on Automatic Control*, Vol.51, No.2, 2006, pp.242-257.

[7] Fradkov, A. and Andrievsky, B., Combined adaptive controller for UAV guidance, *European Journal of Control*, Vol.11, No.1, 2005, pp.71-79.

[8] Kim, M.S. and Chung, C.S., The robust flight control of an UAV using MIMO QFT: GA-based automatic loop-shaping method, *Systems Modeling and Simulation: Theory and Applications Lecture Notes in Computer Science*, No.3398, 2005, pp.467-477.

[9] Singh, S.N., Zhang, R., Chandler, P. and Banda, S., Decentralized nonlinear robust control of UAVs in close formation, *International Journal of Robust and Non-Linear Control*, Vol.13, No.11, 2003, pp.1057-1078.

[10] Lombaerts, T.J.J., Mulder, J.A., Voorsluijs, G.M. and Decuypere, R, Design of a robust flight control system for a mini-UAV, *AIAA Guidance, Navigation, and Control Conference*, Vol.7, 2005, pp.5608-5626.

[11] Chen, Xin and Pan, Changchun, Application of H infinity control and inverse dynamic system in direct side force control of UAV, *Journal of Nanjing University of Aeronautics and Astronautics*, Vol.38, No.1, 2006, pp.33-36.

[12] Sadraey, M. and Colgren, R., Two DOF robust nonlinear autopilot design for a small UAV using a combination of dynamic inversion and H varies directly as loop shaping, *AIAA Guidance, Navigation, and Control Conference*, 2005, pp.5518-5538.

[13] Morari, M., Schaufelberger, W., Glattfelder, A, Christophersen, F.J. and Geyer, T., Analyse und Drehzahlregelung einer flexiblen Welle (LQR Control of a Flexible Shaft), Institut für Automatik Fachpraktikumsversuch IfA 3.1 (Automatic Control Laboratory Experiment 3.1), ETH Zuerich (Swiss Federal Institute of Technology), Switzerland, April 2005.

[14] Blakelock, J. H., *Automatic Control of Aircraft and Missiles*, Wiley, 1991.

[15] Turkoglu, K., Investigation the modes of Hezarfen UAV and automatic control systems design, *B.Sc. Graduation Thesis in Istanbul, Tech. Univ., Faculty of Aeronautics and Astronautics*, Supervised by Prof. E. M. Jafarov, 2006, pp.13-16.

[16] Ogata, K., *Modern Control Engineering*, Prentice Hall, Third Edition, 1997.